BIOCHEMISTRY
including biophysical chemistry & molecular biology

Article

pubs.acs.org/biochemistry

Small Molecule Inhibition of the Na^+/H^+ Exchange Regulatory Factor 1 and Parathyroid Hormone 1 Receptor Interaction

Jeremy M. Fitzpatrick, Maria Pellegrini, Patrick R. Cushing, and Dale F. Mierke*

Department of Chemistry and Department of Molecular and Cellular Biology, Dartmouth College, Hanover, New Hampshire 03755, United States

Supporting Information

ABSTRACT: We have identified a series of small molecules that bind to the canonical peptide binding groove of the PDZ1 domain of NHERF1 and effectively compete with the association of the C-terminus of the parathyroid hormone 1 receptor (PTH1R). Employing nuclear magnetic resonance and molecular modeling, we characterize the mode of binding that involves the GYGF loop important for the association of the C-terminus of PTH1R. We demonstrate that the common core of the small molecules binds to the PDZ1 domain of NHERF1 and displaces a ^{15}N-labeled peptide corresponding to the C-terminus of PTH1R. The small size (molecular weight of 192) of this core scaffold makes it an excellent candidate for further elaboration in the development of an inhibitor for this important protein−protein interaction.

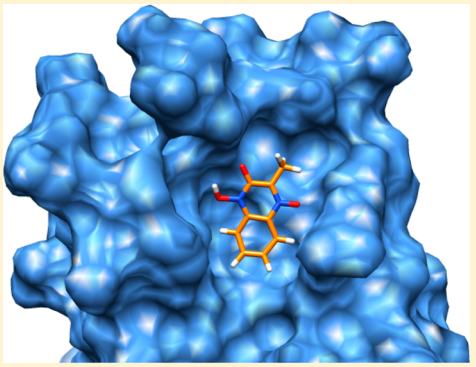

The parathyroid hormone 1 receptor (PTH1R) is a major regulator of serum calcium and phosphate homeostasis and plays an important role in hypercalcemia and osteoporosis.[1−3] Within osteoblasts, the activation of the PTH1R elicits two distinct signaling pathways.[4] One is the protein kinase A (PKA) pathway in which adenylyl cyclase (AC) is stimulated through Gαs,[5] associated with an increase in bone mass.[6] Activation of this pathway by parathyroid hormone (PTH), under the trade name Forteo, has been developed as a treatment for osteoporosis.[7,8] However, the effectiveness of the treatment is limited and requires a precise dosing regimen to maintain its anabolic effect.[9]

In a parallel fashion, the stimulation of PTH1R when it is bound to the molecular scaffolding protein Na^+/H^+ exchange regulatory factor 1 (NHERF1) leads to activation of the protein kinase C (PKC) pathway through phospholipase Cβ (PLCβ).[10] This pathway is associated with catabolic activity; the overstimulation of this pathway is believed to be the cause of bone loss resulting from continuously elevated levels of PTH.[5] However, the presence of NHERF1 and consequential activation of the PKC pathway are important for normal bone growth, as NHERF1 null mice showed a reduction in the rate of bone reabsorption as well as bone formation, resulting in bone that is 25% weaker because of a lack of collagen cross-linking.[11] Hence, while completely eliminating signaling through PLCβ would have deleterious effects on bone health, knocking down its activity through intermittent dosing with a NHERF1 inhibitor may provide improved PTH based therapies.

The selectivity in signaling imparted by NHERF1 is associated with the stabilization of a complex between PTH1R and PLCβ, in which the C-termini of these two transmembrane proteins bind to one of the two PDZ domains of NHERF1. It was originally reported that the C-terminus of PTH1R bound only to the PDZ1 domain of NHERF1, but not to the PDZ2 domain.[12] This observation is likely the result of the C-terminus of NHERF1 binding to the PDZ2 domain in an autoinhibitory fashion.[12] More recent results have shown that the C-terminus of PTH1R is capable of binding to PDZ1 or PDZ2, with equal affinity.[13] Interestingly, this study also demonstrated that binding to the PDZ1 domain (by the C-terminus of either PTH1R or PLCβ) leads to the homodimerization of NHERF1 through the PDZ2 domains.[13] This has led to the model in which a dimer of NHERF1 (formed through the PDZ2 domains) stabilizes the colocalization of PTH1R and PLCβ by binding to their C-termini (through the PDZ1 domains). The resulting protein complex is anchored to the cytoskeleton through interactions with ezrin through the ERM (ezrin, radixin, and moesin) binding motif at the C-terminus of NHERF1.[10]

The PDZ1 domain of NHERF1 is a class I PDZ domain that recognizes the X-(S/T)-X-Φ-COOH sequence, where Φ is a hydrophobic residue. The binding motif for the NHERF1 PDZ1 domain has been further refined to include D/E-(S/T)-X-(L/V/I/M)-COOH.[12,14−16] The four C-terminal amino acids of PTH1R (ETVM) are consistent with this motif. The C-terminus of PLCβ (consisting of DTPL and ESRL for the β1 and β2 isozymes, respectively) has also been shown to bind NHERF1.[13] Interestingly, the C-terminus of PLCβ3 was reported to bind to the PDZ2 domain of NHERF1.[12]

Received: March 26, 2014
Revised: August 29, 2014
Published: August 29, 2014

   dx.doi.org/10.1021/bi500368k | *Biochemistry* 2014, 53, 5916−5922

Here, we aim to identify small molecule inhibitors of the interaction of the C-terminus of PTH1R with the PDZ1 domain of NHERF1. Such a molecule could serve as an important physiological tool for ascertaining the importance of this interaction in the regulation of PTH1R stimulation, possibly providing an avenue to address hypercalcemia. As NHERF1 has been implicated in many cancers, acting as a molecular scaffold in the regulation of transmembrane receptors, an inhibitor could provide valuable insight into the mechanism of action.[17] NHERF1 is also highly expressed in the kidneys where it is linked to renal phosphate wasting,[18] and therefore, a PDZ1 domain specific inhibitor would be a valuable tool. Employing a combination of computational and nuclear magnetic resonance (NMR)-based screening methods, we have identified a number of small molecules that bind to the PDZ1 domain of NHERF1. The experimentally validated hits were tested for their ability to inhibit the interaction of the 17 C-terminal amino acids of PTH1R with the NHERF1 PDZ1 domain using NMR and fluorescence polarization. We further optimized the inhibitor and conducted molecular dynamics (MD) simulations to determine the potential of future derivatives.

EXPERIMENTAL PROCEDURES

Protein Expression and Purification. Human NHERF1 PDZ1 (1−140) was cloned into a pET16 b(+) vector with an N-terminal 10-histidine tag. Unlabeled NHERF1 PDZ1 was expressed by growing a 250 mL culture of BL21 RIL *Escherichia coli*. The culture was induced at an OD_{600} between 0.6 and 0.8 by adding IPTG to a final concentration of 0.1 mM. After induction, the culture was grown at 20 °C for 16−18 h. For ^{15}N-enriched and ^{15}N- and ^{13}C-enriched protein expression, the culture was grown to a density with an OD_{600} between 3 and 4, spun down, and resuspended in minimal medium of equal volume [48 mM Na_2HPO_4, 22 mM KH_2PO_4, 43 mM NaCl, 5 mM $MgSO_4$, 0.2 mM $CaCl_2$, 0.25× metal ion solution, 0.25× BME vitamins, 0.25× thiamine, 3 g/L $^{15}NH_4Cl$, and 10 g/L [^{13}C]glucose (pH 8.0)].[19]

NHERF1 PDZ1 was purified by first pelleting the *E. coli* cells at 4000 rpm for 15 min. Pelleted cells were resuspended in lysis buffer [50 mM Tris, 150 mM NaCl, 10 mM imidazole, 0.02% (w/v) NaN_3, 2 mM $MgCl_2$, 3 μL Benzonase per 50 mL, and 1 Roche protease inhibitor tablet per 50 mL (pH 8.5)]. The resuspended cells were lysed using a French press, at a pressure of 1500 psi. The lysate was spun down at 40000 rpm for 25 min. The supernatant was loaded onto a GE 5 mL HisTrap HP column using an ÄKTAxpress instrument. The column was washed with wash buffer after being loaded until a steady baseline was reached (absorbance of 280 nm). The wash buffer consisted of 50 mM Tris, 150 mM NaCl, 0.02% (w/v) NaN_3, and 10 mM imidazole (pH 8.5). A 20 column volume gradient of elution buffer was used to elute NHERF1 PDZ1. Fractions (1.8 mL) of the elutant were collected. The elution buffer was the same with 400 mM imidazole. Fractions containing NHERF1 PDZ1, as determined by sodium dodecyl sulfate−polyacrylamide gel electrophoresis analysis, were further purified through size exclusion chromatography using an ÄKTA purifier with a Superdex 75 16/60 column. The size exclusion buffer was the same as the wash buffer used for the 5 mL HisTrap column purification, without imidazole. The fractions containing NHERF1 PDZ1 were concentrated using 10000 molecular weight cutoff centrifugal concentrators, spinning at 3000*g* and mixing at intervals of 15 min. Protein that was to be frozen for later use was dialyzed into 25 mM sodium phosphate, 150 mM NaCl, 0.1 mM TCEP, 0.02% (w/v) NaN_3, and 5% (v/v) glycerol (pH 7.4). A reading of absorbance at 280 nm was used to quantify NHERF1 PDZ1 with an extinction coefficient of 2464 M^{-1} cm^{-1}, as determined by Keck MS and Proteomics Resources at Yale University (New Haven, CT).

The C-terminal 17-amino acid peptide of human PTH1R (GPERPPALLQEEWETVM) was expressed with a N-terminal thirodoxin (Trx) tag in a pET32a vector.[20] A tobacco etch virus (TEV) protease cleavage site was inserted between the Trx tag and peptide. After cleavage by the TEV protease, only the 17 C-terminal amino acids of human PTH1R (PTH1Rct) remained. A detailed description of the production and NMR assignment of the peptide was published previously.[21]

NMR Experiments. Experiments for ligand binding analysis and titrations to determine K_D values were conducted on a Bruker Avance III 700 MHz NMR instrument, equipped with a 5 mm TCI cryoprobe. All experiments were conducted at 298 K. Samples for initial ligand screening used a concentration of 50 μM NHERF1 PDZ1 (1−140) and 2 mM ligand, in a buffer consisting of 25 mM sodium phosphate, 50 mM NaCl, 0.1 mM TCEP, 0.02% (w/v) NaN_3, 1% (v/v) DMSO-d_6, and 5% (v/v) D_2O (pH 6.8). For ^{1}H−^{15}N HSQC experiments, 16 scans were collected with 1024 points in the ^{1}H dimension and 128 in the ^{15}N dimension. Ligand K_D values were determined using the same method except that the buffer contained 2.5% (v/v) DMSO-d_6. The ligand concentrations used for the titration were 0, 0.33, 0.67, 1, 2, 3, 4, and 5 mM. ^{1}H−^{15}N HSQC spectra were processed using Topspin and analyzed using Sparky 3.115.[22] The chemical shift perturbation was calculated using eq 1.[23]

$$\Delta_{obs} = \sqrt{\frac{\Delta_{^1H}{}^2 + \left(\frac{\Delta_{^{15}N}}{5}\right)^2}{2}} \quad (1)$$

where Δ_{obs} is the normalized chemical shift, $\Delta_{^1H}$ is the change in the chemical shift in the ^{1}H dimension, and $\Delta_{^{15}N}$ is the change in the chemical shift in the ^{15}N dimension.

Analysis of the normalized peak shift values was conducted in Kaleidagraph 4.01, and eq 2 was used to determine K_d values.[24]

$$\Delta_{obs} = \frac{\Delta_{max}[K_d + L + P - \sqrt{(K_d + L + P)^2 - 4PL}\,]}{2P} \quad (2)$$

where Δ_{obs} is the observed change in the chemical shift, Δ_{max} is the chemical shift when the protein is completely saturated with ligand, L is the ligand concentration, and P is the protein concentration.

The competition binding experiments were conducted on a Bruker Avance III 600 MHz NMR instrument, equipped with a 1.7 mm cryoprobe. The control sample consisted of 75 μM unlabeled NHERF1 PDZ1 with 30 μM ^{15}N-labeled PTH1R C-terminus, in a buffer that consisted of 25 mM sodium phosphate, 50 mM NaCl, 0.1 mM TCEP, 0.02% (w/v) NaN_3, 5% (v/v) DMSO-d_6, and 5% (v/v) D_2O (pH 6.8). DMSO-d_6 was used to solubilize the core-CH_3 for addition to the sample. For ^{1}H−^{15}N HSQC experiments, 16 scans were collected with 1024 points in the ^{1}H dimension and 128 in the ^{15}N dimension. The assignment of NHERF1 PDZ1 will be detailed in a separate publication and was deposited in the BMRB as entry 19781.

dx.doi.org/10.1021/bi500368k | *Biochemistry* 2014, 53, 5916−5922

Fluorescence Polarization Assay. Fluorescence polarization (FP) measurements were taken on a Tecan Infinity 500 plate reader. All experiments were conducted at 298 K in triplicate. Data were processed using Kaleidagraph 4.01. The buffer used for the FP assay consisted of 25 mM sodium phosphate, 150 mM NaCl, 0.2 mM TCEP, 0.02% (w/v) NaN_3, 0.5 mM Thesit, and 0.1 mg/mL IgG (pH 7.4). The 16 fluorescently tagged C-terminal amino acids of PTH1R [FITC]β_aPERPPALLQEEWETVM (FITC-PTH1Rct) were used for the assay. For all experiments, the concentration of FITC-PTH1Rct was 30 nM. For the competition experiment, a NHERF1 PDZ1 (1−140) concentration of 19 μM was used. K_D was calculated using eq 3.[25]

$$\text{FP reading} = \text{FP}_{\text{min}} + (\text{FP}_{\text{max}} - \text{FP}_{\text{min}}) \frac{L + K_D + P - \sqrt{(L + K_D + P)^2 - 4LP}}{2L} \quad (3)$$

where FP_{min} is the FP value when no ligand is bound, FP_{max} is the FP value when all ligand is bound, L is the ligand concentration, and P is the protein concentration.

To determine the IC_{50} value, we applied a four-parameter logistics function (see eq 4).[26]

$$\text{FP reading} = \text{FP}_{\text{min}} + \frac{\text{FP}_{\text{max}} - \text{FP}_{\text{min}}}{1 + \left[\frac{\log(L)}{\log(\text{IC}_{50})}\right]^A} \quad (4)$$

where FP_{min} is the value when no ligand is bound, FP_{max} is the FP value when all ligand is bound, IC_{50} is the concentration of ligand at which half the peptide binding is inhibited, and A is the slope factor.

Library Screening. For computational screening, we used the apo-NHERF1 PDZ1 structure available from the Protein Data Bank (PDB) (entry 1G9O)[27] and a 3000-compound diversity library developed from Life Chemicals. The screenings were conducted using Molecular Operating Environment 2012.10.[28] Ligands were docked into the canonical peptide binding groove of NHERF1 PDZ1, including the GYGF loop.[29] "Triangle Matcher" was used for the placement of ligands and "London dG" for the scoring of ligands.

To generate a model of core-CH_3 binding to the PDZ domain, we used Autodock 4.0.[30] The structures resulting from Autodock that were in agreement with the chemical shift perturbation data from NMR were selected for further refinement via molecular dynamics (MD) simulations. We used the energy-minimized 1G9O structure [using NAMD (see below)] and the default docking parameters, with the following exceptions: ga_pop_size = 300 and ga_run = 256. It has been noted that increasing the ga_pop_size up to 300 improves the results from docking.[31] The ligand efficiency of the docking results was calculated using eq 5.[32]

$$\text{LE} = \Delta G/N \quad (5)$$

where LE is the ligand efficiency, ΔG is the Gibbs free energy, and N is the number of non-hydrogen atoms.

Energy minimization and MD simulations were conducted with NAMD 2.9.[33] Input files were generated using VMD 1.9.1, psfgen 1.6, and solvate 1.5. The simulation box (48.4 Å × 48.0 Å × 43.4 Å) was solvated with TIP3P water with Na^+ and Cl^- ions added to neutralize the system.[34] Structures were energy minimized for 50000 steps (0.1 ns), followed by 2500000 steps (5 ns) of MD (step size of 2 fs) at 300 K and 1.01 bar. Identical MD simulations were conducted with the methyl group of core-CH_3 replaced by the following groups: $-CH_2CH_3$, $-CH(CH_3)_2$, $-C(CH_3)_3$, $-CH_2CH_2CH_3$, $-CH_2CH_2CH_2CH_3$, and $-CH_2CH_2CH_2CH_2CH_3$. Analysis of hydrogen bonding was conducted in VMD 1.9.1, using the parameters of a N−O distance of 3.5 Å and an angle of 90°. Hydrogen bond analysis was limited to the last 3.5 ns of the simulation, after equilibrium had been reached. Figures were created using Chimera 1.6.1.[35]

RESULTS

Of the 10 lowest-energy structures from our computational screen of the 3000-compound library, nine were commercially available and therefore examined experimentally (Figure 1 of the Supporting Information). On the basis of the chemical shift perturbation of the assigned $^1H-^{15}N$ HSQC NMR spectrum of NHERF1 PDZ1 (Figure 1), only one (F0911−3941) bound

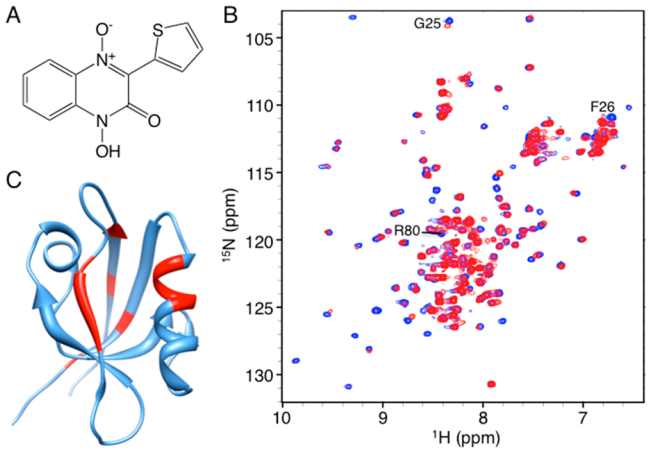

Figure 1. F0911−3941 binding to NHERF1 PDZ1. (A) Structure of compound F0911−3941. (B) $^1H-^{15}N$ HSQC spectra of ^{15}N-labeled NHERF1 PDZ1 at a concentration of 50 μM (blue) and in the presence of 1 mM F0911−3941 (red). (C) Mapping of residues (red) that undergo a significant perturbation (more than one standard deviation removed from the mean shift) upon binding of F0911−3941, using the X-ray structure of NHERF1 PDZ1 (PDB entry 1G9O).

(see Figure 2 of the Supporting Information for all chemical shift perturbations). Mapping of the chemical shift perturbations onto the structure of the PDZ domain clearly demonstrates that the compound is binding in the canonical peptide binding groove and interacting with the GYGF loop (Figure 1C). Note that the construct used for our NMR experiments contained NHERF1(1−140), which is necessary to enhance solution stability, while the X-ray structure (PDB entry 1G90) used in our modeling, and in the figures, consists of only NHERF1(9−99). Importantly, in all of our NMR experiments, there was no evidence that the extra amino acids interacted with any of the peptides or small molecules that were examined.

The ability of F0911−3941 to inhibit the interaction of PTH1Rct with NHERF1 PDZ1 was examined by fluorescence polarization experiments. We observed that FITC-labeled PTH1Rct bound to NHERF1 PDZ1 with an affinity of 19 ± 2 μM (see Figure 3 of the Supporting Information). A K_D value of 11 μM had previously been reported in the literature.[13] With a PDZ1 concentration of 9 μM and the FITC-tagged PTH1Rct at a concentration of 30 nM, we observed an IC_{50} of 50 ± 5 μM

dx.doi.org/10.1021/bi500368k | Biochemistry 2014, 53, 5916−5922

for F0911−3941 (Figure 2). This value is likely a low estimate given the amount of NHERF1 PDZ1 used in the experiment was only sufficient for 33% occupancy.

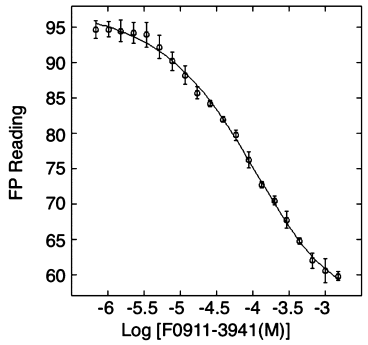

Figure 2. Inhibition of the binding of PTH1Rct to PDZ1 of NHERF1. Compound F0911−3941 competes for the binding of the C-terminus of PTH1R to the PDZ1 domain of NHERF1 with an IC_{50} value of 50 ± 5 μM.

To develop a structure−activity relationship for F0911−3941, we searched the ZINC database for small molecules that were 50% structurally similar.[36] This search yielded 1272 compounds. Using computational docking, these compounds were examined for their ability to bind to NHERF1 PDZ1. Of the 10 lowest-energy hits, eight were commercially available and examined for binding by NMR (see Figure 4 and Table 1 of the Supporting Information). On the basis of chemical shift perturbation, all eight compounds were found to bind to the GYGF loop of NHERF1 PDZ1 in a manner similar to that of F0911−3941. However, given the low affinity of these compounds, as measured by NMR (Table 1 of the Supporting Information), they were not pursued further.

As an alternative approach, we asked if the central core scaffold of F0911−3941 (denoted as core-CH_3) displayed any affinity for NHERF1 PDZ1. In Figure 3B, a superposition of the $^1H-^{15}N$ HSQC spectra of NHERF1 PDZ1 with and without the core-CH_3 structure is shown, clearly demonstrating binding within the canonical peptide binding groove and interaction with the GYGF loop (see Figure 5 of the Supporting Information for a graph of all chemical shift perturbations). The mapping of the chemical shift perturbation (one standard deviation above the average) onto the X-ray structure of PDZ1 is shown in Figure 3C. Next we tested the ability of core-CH_3 to inhibit the interaction of PTH1Rct with NHERF1 PDZ1. Unfortunately, core-CH_3 has an absorbance profile that makes it unsuitable for FP experiments. We therefore turned to NMR employing an ^{15}N-labeled PTH1Rct, which allowed us to observe the peptide while free and while bound to PDZ1. With a sample of 30 μM [^{15}N]PTH1Rct as a starting point (the free spectrum), 75 μM natural abundance NHERF1 PDZ1 was added providing the bound spectrum. As shown in Figure 4A, many of the peptide peaks are broadened

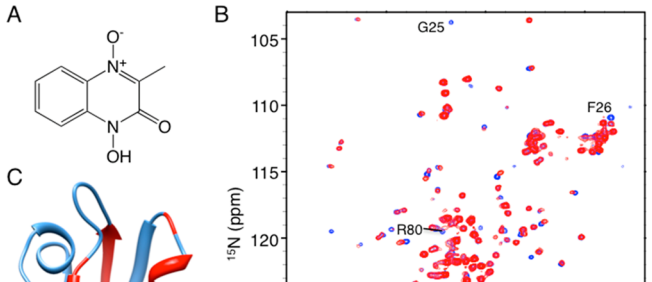

Figure 3. Core-CH_3 and its interaction with NHERF1 PDZ1. (A) Structure of the common core scaffold of the small molecules shown to bind to NHERF1 PDZ1. (B) $^1H-^{15}N$ HSQC spectra of NHERF1 PDZ1 alone (blue) and in the presence of the core-CH_3 compound (red). (C) Mapping (using the X-ray structure of PDB entry 1G9O) of the residues (red) within PDZ1 that are shifted by more than one standard deviation from the mean or are broadened below the noise level.

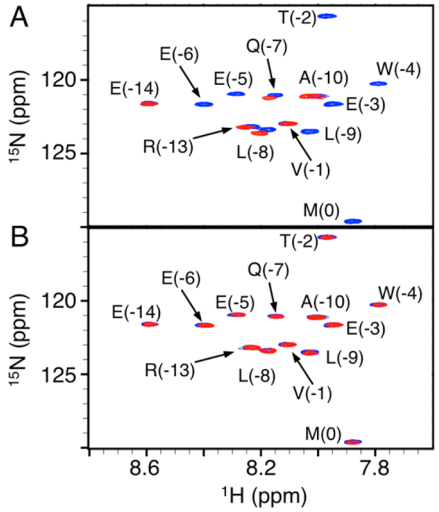

Figure 4. Interaction and inhibition of the binding of PTH1Rct to NHERF1 PDZ1. (A) $^1H-^{15}N$ HSQC spectra of ^{15}N-labeled PTH1Rct alone (blue) and bound to the PDZ1 domain (red). (B) In the presence of core-CH_3 (red), the resonances of ^{15}N-labeled PTH1Rct return back to their values when it is free (blue).

below the noise when it is bound to NHERF1 PDZ1. Upon the addition of core-CH_3, the spectrum of the peptide moves toward the unbound state (see Figure 4B). Using a conservative estimate that 95% of NHERF1 PDZ1 is bound to core-CH_3, an approximate K_D of ≤300 μM can be calculated for the binding of core-CH_3 to NHERF1 PDZ1.

To obtain greater insight into the interaction of core-CH_3 with NHERF1 PDZ1, docking and MD simulations were conducted. From AutoDock, the lowest-energy complex conformation had a ΔG of −6.07 kcal mol^{-1}, resulting in a ligand efficiency of 0.43 kcal mol^{-1} heavy $atom^{-1}$ for core-CH_3. The subsequent MD simulations demonstrated that this was a stable structure with a number of hydrogen bonds between core-CH_3 and Y24 and G25 (Figure 5). Additionally, during the simulations, there is a shift in β-strand 2 of NHERF1 PDZ1, as a result of core-CH3 binding, consistent with the chemical shift perturbations in β-strand 2 upon binding. The amide resonance of G25 is broadened below the noise level, suggesting an interaction with core-CH_3. Unfortunately, Y24 was not identified during our resonance assignment. We believe that ligand binding may also have some long-range effects on β2 and

dx.doi.org/10.1021/bi500368k | *Biochemistry* 2014, 53, 5916−5922

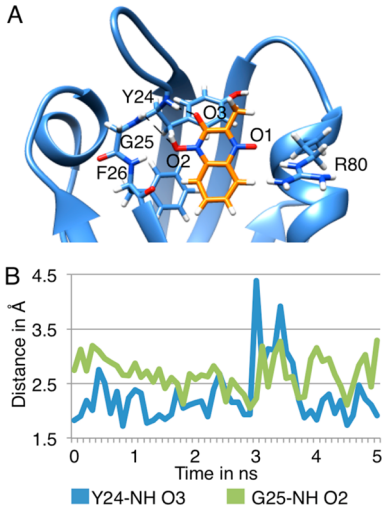

Figure 5. Molecular dynamics simulation of binding of core-CH_3 to NHERF1 PDZ1. (A) Final structure of core-CH_3 (orange) with NHERF1 PDZ1 (blue) after a 5 ns MD simulation. Potential hydrogen bonds are shown as dashed lines. Residues Y24 and G25 were shown to interact with core-CH_3 during the simulation. Although F26 and R80 did not appear to interact significantly with core-CH_3 during the simulation, they did show significant chemical shift perturbation. (B) Plot of the distances between the amide proton of Y24 and O3 (blue) and between G25 and O2 (green).

helix α2. A superposition of the NHERF1 PDZ1 structure before and after the MD simulation is provided as Figure 6 of the Supporting Information.

To examine the possibility of functionalizing the core, we conducted additional MD simulations. Given the hydrophobic nature of the pocket, we restricted the search of substituent groups to hydrocarbons. The methyl of the core was replaced with the following R groups: -$C(CH_3)_3$, -$CH(CH_3)_2$, -CH_2CH_3, -$CH_2CH_2CH_3$, -$CH_2CH_2CH_2CH_3$, and -$CH_2CH_2CH_2CH_2CH_3$. We observed that any R group with more than three carbons was not well tolerated within the binding pocket; there were multiple steric clashes, requiring significant conformational changes of helix α2 that were energetically unfavorable. However, the compounds containing the R groups -$C(CH_3)_3$, -$CH(CH_3)_2$, -CH_2CH_3, and -CH_3 were all found to be energetically favorable based on the MD simulations (see Figure 7 of the Supporting Information).

DISCUSSION

More than 150 human proteins containing at least one PDZ domain have been identified. The PDZ domain binds to the C-terminus of its partner proteins, often in the role of a molecular scaffold. As such, the PDZ domains are designed to enhance the local concentrations of the interacting proteins, bringing them into the proximity of each other to facilitate an interaction that is transient and not designed to be long-lived.[37,38] Consistent with this physiological role, the binding affinities for PDZ domains are typically in the low micromolar range. Accordingly, the binding pocket of PDZ domains is shallow and relatively nondescript with very few points of interaction,[29,37] and therefore, the interactions of PDZ domains with their targets are typically difficult to inhibit.[39,40]

Although it is a difficult task, there have been some successes in inhibiting the interactions with PDZ domains reported within the literature. Interestingly, most of the successful compounds are based on an indole scaffold,[39−42] including a compound that has been shown to bind to NHERF1 and inhibit the interaction with the C-terminus of cystic fibrosis transmembrane regulator.[39] In contrast, we present a novel inhibitor, characterized by a quinoxaline core. Another striking difference between our inhibitor and the previous small molecules is the manner in which they target the GYGF loop: most of the compounds previously reported contain a carboxyl group to interact with the GYGF loop, in a fashion analogous to that of the C-terminus of the naturally occurring peptides. In contrast, the compound presented here interacts with the carboxylate binding loop via a hydroxyl group and a carbonyl within the ring system (Figure 5A). A similar interaction has been presented by Thorsen et al. in which an acryoylcarbamate inhibitor interacts with the GYGF loop via a dichlorophenyl group instead of a carboxylic acid.[43] A significant advantage of the compound presented here is the small size; the molecular weight of our core compound is only 192, but it still maintains a micromolar IC_{50}. Most of the compounds presented previously are much larger while still providing IC_{50} values in the micromolar range.

Future efforts will focus on defining the regions of the molecule that can be modified to enhance the affinity. On the basis of the refined complex structure (Figure 5A), the replacement of O1 with an aldehyde or methyl hydroxyl would allow for hydrogen bonds with the side chain of R80 while simultaneously maintaining the hydrogen bonds between O2 and O3 and the backbone of the GYGF loop. Another potential improvement targets the small lipophilic side chains at the position of the methyl in core-CH_3 (see Figure 7 of the Supporting Information). On the basis of our preliminary simulations, small modifications are feasible and may provide additional interaction with the PDZ1 domain and thereby enhance affinity. Following along the lines of the acryoylcarbamate inhibitor of Thorsen et al.,[43] we can envision addition of substitutions to the benzene ring that would provide additional interactions within the peptide binding groove.

In conclusion, core-CH_3 identified here binds to the PDZ1 domain of NHERF1 and competes with the binding of the C-terminus of PTH1R. The potency of the inhibitor is in line with those of other PDZ inhibitors reported in the literature, but the small molecule has the advantage of a low molecular weight, allowing for further elaboration to increase its binding affinity. Further modifications would certainly be required for specificity. Indeed, given the mode of binding proposed here, we postulate that core-CH_3 will bind to PDZ2 of NHERF1 given that all of the main interactions are with the backbone of the GYGF loop, a feature maintained by both PDZ domains of NHERF1 and many other PDZ domains. Efforts to enhance the affinity and specificity by the elaboration of core-CH_3 as outlined here are currently underway.

ASSOCIATED CONTENT

Supporting Information

Figures 1−7. This material is available free of charge via the Internet at http://pubs.acs.org.

AUTHOR INFORMATION

Corresponding Author

*Dartmouth College, 41 N. College St., Hanover, NH 03755. E-mail: dale.f.mierke@dartmouth.edu. Telephone: (603) 646-1154. Fax: (603) 646-3946.

Funding

Funding was provided by the National Institutes of Health Grants R01-DK075309 and GM082054 as well as a grant from the Molecular and Cellular Biology training program at Dartmouth College (T32-GM008704).

Notes

The authors declare no competing financial interest.

■ ABBREVIATIONS

NHERF1, Na^+/H^+ exchange regulatory factor 1; PLCβ, phospholipase Cβ; PTH1R, parathyroid hormone 1 receptor; PDZ, post-synaptic density protein 95, drosophila disc large tumor suppressor 1, zonula occludens-1 protein; PTH, parathyroid hormone; PTHrP, parathyroid hormone-related peptide; AC, adenylyl cyclase; PTH1Rct, 16 residues of the C-terminus of the parathyroid hormone 1 receptor; β_a, β-alanine; PKA, protein kinase A; PKC, protein kinase C.

■ REFERENCES

(1) Weinman, E. J., and Lederer, E. D. (2012) NHERF-1 and the regulation of renal phosphate reabsoption: A tale of three hormones. *Am. J. Physiol. 303*, F321−F327.

(2) Lederer, E. D. (2003) Role of NHERF-1 in Regulation of the Activity of Na-K ATPase and Sodium-Phosphate Co-transport in Epithelial Cells. *J. Am. Soc. Nephrol. 14*, 1711−1719.

(3) Voltz, J. W., Weinman, E. J., and Shenolikar, S. (2001) Expanding the role of NHERF, a PDZ-domain containing protein adapter, to growth regulation. *Oncogene 20*, 6309−6314.

(4) Datta, N. S., and Abou-Samra, A. B. (2009) PTH and PTHrP signaling in osteoblasts. *Cell. Signalling 21*, 1245−1254.

(5) Qin, L., Raggatt, L. J., and Partridge, N. C. (2004) Parathyroid hormone: A double-edged sword for bone metabolism. *Trends Endocrinol. Metab. 15*, 60−65.

(6) Rixon, R. H., Whitfield, J. F., Gagnon, L., Isaacs, R. J., Maclean, S., Chakravarthy, B., Durkin, J. P., Neugebauer, W., Ross, V., and Sung, W. (1994) Parathyroid hormone fragments may stimulate bone growth in ovariectomized rats by activating adenylyl cyclase. *J. Bone Miner. Res. 9*, 1179−1189.

(7) Abou-Samra, A.-B., Jüppner, H., Force, T., Freeman, M. W., Kong, X.-F., Schipani, E., Urena, P., Richards, J., Bonventre, J. V., and Potts, J. T. (1992) Expression cloning of a common receptor for parathyroid hormone and parathyroid hormone-related peptide from rat osteoblast-like cells: A single receptor stimulates intracellular accumulation of both cAMP and inositol trisphosphates and increases intracellular free calcium. *Proc. Natl. Acad. Sci. U.S.A. 89*, 2732−2736.

(8) Datta, N. S., Samra, T. A., and Abou-Samra, A. B. (2012) Parathyroid hormone induces bone formation in phosphorylation-deficient PTHR1 knockin mice. *Am. J. Physiol. 302*, E1183−E1188.

(9) Locklin, R. M., Khosla, S., Turner, R. T., and Riggs, B. L. (2003) Mediators of the biphasic responses of bone to intermittent and continuously administered parathyroid hormone. *J. Cell. Biochem. 89*, 180−190.

(10) Mahon, M. J., and Serge, G. V. (2004) Stimulation by Parathyroid Hormone of a NHERF-1-assembled Complex Consisting of the Parathyroid Hormone I Receptor, Phospholipase C, and Actin Increases Intracellular Calcium in Opossum Kidney Cells. *J. Biol. Chem. 279*, 23550−23558.

(11) Liu, L., Alonso, V., Guo, L., Tourkova, I., Henderson, S. E., Almarza, A. J., Friedman, P. A., and Blair, H. C. (2012) Na^+/H^+ exchanger regulatory factor 1 (NHERF1) directly regulates osteogenesis. *J. Biol. Chem. 287*, 43312−43321.

(12) Mahon, M. J., and Segre, G. V. (2004) Stimulation by parathyroid hormone of a NHERF-1-assembled complex consisting of the parathyroid hormone I receptor, phospholipase Cβ, and actin increases intracellular calcium in opossum kidney cells. *J. Biol. Chem. 279*, 23550−23558.

(13) Sun, C., and Mierke, D. F. (2005) Characterization of interactions of Na^+/H^+ exchanger regulatory factor-1 with the parathyroid hormone receptor and phospholipase C*. *J. Pept. Res. 65*, 411−417.

(14) Doyle, D. A., Lee, A., Lewis, J., Kim, E., Sheng, M., and MacKinnon, R. (1996) Crystal structures of a complexed and peptide-free membrane protein-binding domain: Molecular basis of peptide recognition by PDZ. *Cell 85*, 1067−1076.

(15) Bhattacharya, S., Ju, J. H., Orlova, N., Khajeh, J. A., Cowburn, D., and Bu, Z. (2013) Ligand-induced dynamic changes in extended PDZ domains from NHERF1. *J. Mol. Biol. 425*, 2509−2528.

(16) Akabas, M. H. (2000) Cystic fibrosis transmembrane conductance regulator: Structure and function of an epithelial chloride channel. *J. Biol. Chem. 275*, 3729−3732.

(17) Georgescu, M.-M., Morales, F. C., Molina, J. R., and Hayashi, Y. (2008) Roles of NHERF1/EBP50 in cancer. *Curr. Mol. Med. 8*, 459−468.

(18) Shenolikar, S., Voltz, J. W., Minkoff, C. M., Wade, J. B., and Weinman, E. J. (2002) Targeted disruption of the mouse NHERF-1 gene promotes internalization of proximal tubule sodium-phosphate cotransporter type IIa and renal phosphate wasting. *Proc. Natl. Acad. Sci. U.S.A. 99*, 11470−11475.

(19) Sivashanmugam, A., Murray, V., Cui, C., Zhang, Y., Wang, J., and Li, Q. (2009) Practical protocols for production of very high yields of recombinant proteins using *Escherichia coli*. *Protein Sci. 18*, 936−948.

(20) Lavallie, E. R., DiBlasio, E. A., Kovacic, S., Grant, K. L., Schendel, P. F., and McCoy, J. M. (1993) A Thioredoxin Gene Fusion Expression System That Circumvents Inclusion Body Formation in the *E. coli* Cytoplasm. *Nat. Biotechnol. 11*, 187−193.

(21) Audu, C. O., Cochran, J. C., Pellegrini, M., and Mierke, D. F. (2013) Recombinant production of TEV cleaved human parathyroid hormone. *J. Pept. Sci. 19*, 504−510.

(22) Goddard, T. D., and Kneller, D. G. *SPARKY 3*, University of California, San Francisco.

(23) Banaszynski, L. A., Liu, C. W., and Wandless, T. J. (2005) Characterization of the FKBP·Rapamycin·FRB Ternary Complex. *J. Am. Chem. Soc. 127*, 4715−4721.

(24) Fielding, L. (2007) NMR methods for the determination of protein−ligand dissociation constants. *Prog. Nucl. Magn. Reson. Spectrosc. 51*, 219−242.

(25) Cushing, P. R., Fellows, A., Villone, D., Boisguérin, P., and Madden, D. R. (2008) The Relative Binding Affinities of PDZ Partners for CFTR: A Biochemical Basis for Efficient Endocytic Recycling. *Biochemistry 47*, 10084−10098.

(26) Wang, Z.-X. (1995) An exact mathematical expression for describing competitive binding of two different ligands to a protein molecule. *FEBS Lett. 360*, 111−114.

(27) Karthikeyan, S., Leung, T., Birrane, G., Webster, G., and Ladias, J. A. (2001) Crystal structure of the PDZ1 domain of human Na^+/H^+ exchanger regulatory factor provides insights into the mechanism of carboxyl-terminal leucine recognition by class I PDZ domains. *J. Mol. Biol. 308*, 963−973.

(28) *Molecular Operating Environment (MOE)*, version 2012.10 (2012) Chemical Computing Group Inc., Montreal.

(29) Mamonova, T., Kurnikova, M., and Friedman, P. A. (2012) Structural basis for NHERF1 PDZ domain binding. *Biochemistry 51*, 3110−3120.

(30) Morris, G. M., Goodsell, D. S., Halliday, R. S., Huey, R., Hart, W. E., Belew, R. K., and Olson, A. J. (1998) Automated docking using a Lamarckian genetic algorithm and an empirical binding free energy function. *J. Comput. Chem. 19*, 1639−1662.

(31) Hetényi, C., and van der Spoel, D. (2002) Efficient docking of peptides to proteins without prior knowledge of the binding site. *Protein Sci. 11*, 1729−1737.

(32) Abad-Zapatero, C. (2007) Ligand efficiency indices for effective drug discovery. *Expert Opin. Drug Discovery 2*, 4.

(33) Phillips, J. C., Braun, R., Wang, W., Gumbart, J., Tajkhorshid, E., Villa, E., Chipot, C., Skeel, R. D., Kalé, L., and Schulten, K. (2005)

Scalable molecular dynamics with NAMD. *J. Comput. Chem. 26*, 1781−1802.
(34) Humphrey, W., Dalke, A., and Schulten, K. (1996) VMD: Visual molecular dynamics. *J. Mol. Graphics 14*, 33−38.
(35) Pettersen, E. F., Goddard, T. D., Huang, C. C., Couch, G. S., Greenblatt, D. M., Meng, E. C., and Ferrin, T. E. (2004) UCSF Chimera: A visualization system for exploratory research and analysis. *J. Comput. Chem. 25*, 1605−1612.
(36) Irwin, J. J., Sterling, T., Mysinger, M. M., Bolstad, E. S., and Coleman, R. G. (2012) ZINC: A Free Tool to Discover Chemistry for Biology. *J. Chem. Inf. Model. 52*, 1757−1768.
(37) Lee, H.-J., and Zheng, J. J. (2010) PDZ domains and their binding partners: Structure, specificity, and modification. *Cell Commun. Signaling 7*, 20.
(38) Fanning, A. S., and Anderson, J. M. (1996) Protein−protein interactions: PDZ domain networks. *Curr. Biol. 6*, 1385−1388.
(39) Mayasundari, A., Ferreira, A. M., He, L., Mahindroo, N., Bashford, D., and Fujii, N. (2008) Rational design of the first small-molecule antagonists of NHERF1/EBP50 PDZ domains. *Bioorg. Med. Chem. Lett. 18*, 942−945.
(40) Fujii, N., Haresco, J. J., Novak, K. A., Gage, R. M., Pedemonte, N., Stokoe, D., Kuntz, I. D., and Guy, R. K. (2007) Rational design of a nonpeptide general chemical scaffold for reversible inhibition of PDZ domain interactions. *Bioorg. Med. Chem. Lett. 17*, 549−552.
(41) Zang, W., Penmatsa, H., Ren, A., Punchihewa, C., Lemoff, A., Yan, B., Fujii, N., and Naren, A. (2011) Functional regulation of cystic fibrosis transmembrane conductance regulator-containing macromolecular complexes: A small-molecule inhibitor approach. *Biochem. J.*, 451−462.
(42) Fujii, N., Haresco, J. J., Novak, K. A., Stokoe, D., Kuntz, I. D., and Guy, R. K. (2003) A selective irreversible inhibitor targeting a PDZ protein interaction domain. *J. Am. Chem. Soc. 125*, 12074−12075.
(43) Thorsen, T. S., Madsen, K. L., Rebola, N., Rathje, M., Anggono, V., Bach, A., Moreira, I. S., Stuhr-Hansen, N., Dyhring, T., Peters, D., Beuming, T., Huganir, R., Weinstein, H., Mulle, C., Strømgaard, K., Rønn, L. C. B., and Gether, U. (2010) Identification of a small-molecule inhibitor of the PICK1 PDZ domain that inhibits hippocampal LTP and LTD. *Proc. Natl. Acad. Sci. U.S.A. 107*, 413−418.